

lower scale height of the atmosphere. The properties of the dust layer must be latitude dependent in the sense that its optical thickness must decrease toward the southern polar region.

The television experiment on Mariner 9 has shown that the southern polar region, as well as certain other isolated areas of Mars, are relatively clear of obscuration by the dust. The residual polar cap is the most well defined feature observed in the thermal scans of Mars, and typically appears 35°K colder than the surrounding terrain.

At the surface of Mars, solid CO₂ must be at its saturated-vapor equilibrium temperature of 148°K. This temperature was observed by Mariner 7 for the south polar cap during the early Martian spring, indicating that the bright deposit was predominantly frozen CO₂ at that time. In contrast, the minimum brightness temperature observed by the Mariner 9 radiometer over the shrinking south polar cap, slightly after Martian southern midsummer, is at least 25°K above the temperature that would correspond to frozen CO₂. From television images obtained simultaneously with the radiometer measurements, the observations correspond to an area at least 95 percent of which is covered with a high albedo deposit.

If the cap is frozen CO₂, these data can be taken to indicate significant emission from the dusty atmosphere. The infrared optical thickness cannot, however, exceed unity as temperature variations have been observed which correlate with sharp features seen in visual images. The net amount of particulate matter required to produce the needed opacity is on the order of 1 mg cm⁻² if its absorption coefficient is typical of silicates in the 10-μm range (2). The possibility that some or all of the residual deposit is now frozen water cannot be excluded on the basis of these data alone.

The southernmost dark feature in Tharsis, at latitude ~11°, longitude ~119°W, also revealed on television images (3), was recognized by the radiometer as a region of about 300 km in length with a temperature about 8°K warmer than its surroundings. A straightforward interpretation of this phenomenon is that locally the atmosphere is more transparent, allowing increased energy to be absorbed by a darker surface. It is of interest to note that near this point radar topographic mapping (4) shows an apparent ridge about 8 km higher than the mean elevation of Mars at this latitude. This pro-

vides a measure of the height of the effective dust layer.

Further analysis of the data is necessary to substantiate these preliminary interpretations.

S. C. CHASE, JR., H. HATZENBELER*
Santa Barbara Research Center,
Goleta, California 93017

H. H. KIEFFER
Department of Planetary and Space
Science, University of California,
Los Angeles 90024

E. MINER
Jet Propulsion Laboratory,
California Institute of Technology,
Pasadena 91103

G. MÜNCH, G. NEUGEBAUER
California Institute of Technology,
Pasadena 91109

References and Notes

1. G. Neugebauer, G. Münch, H. Kieffer, S. C. Chase, Jr., E. Miner, *Astron. J.* **76**, 719 (1971); S. Chase, Jr., E. Miner, G. Münch, G. Neugebauer, *Icarus* **12**, 46 (1970).
2. J. M. Hunt, M. P. Wisherd, L. C. Bonham, *Anal. Chem.* **22**, 1478 (1950); T. Wentink and W. G. Planet, *J. Opt. Soc. Amer.* **51**, 595 (1961).
3. H. Masursky *et al.*, *Science* **175**, 295 (1972).
4. G. H. Pettengill, A. E. E. Rogers, I. I. Shapiro, *ibid.* **174**, 1321 (1971); G. S. Downs R. M. Goldstein, R. R. Green, G. A. Morris, *ibid.*, p. 1324.
5. We thank the personnel of the entire Mariner 9 project for their substantial efforts in our behalf, and the staff of Santa Barbara Research Center for assistance during construction and calibration of the instrument. We also thank J. Bennett, A. Law, B. Eenigenburg, R. Newell, J. Otte, M. Sander, and D. Schofield for their work with this experiment, and R. B. Leighton for his discussion of this report.

* Deceased.

27 December 1971

Mariner 9 Ultraviolet Spectrometer

Experiment: Initial Results

Abstract. *The ultraviolet airglow spectrum of Mars has been measured from an orbiting spacecraft during a 30-day period in November–December 1971. The emission rates of the carbon monoxide Cameron and fourth positive bands, the atomic oxygen 1304-angstrom line and the atomic hydrogen 1216-angstrom line have been measured as a function of altitude. Significant variations in the scale height of the CO Cameron band airglow have been observed during a period of variable solar activity; however, the atomic oxygen and hydrogen airglow lines are present during all the observations. Measurements of the reflectance of the lower atmosphere of Mars show the spectral characteristics of particle scattering and a magnitude that is about 50 percent of that measured during the Mariner 6 and 7 experiments in 1969. The variation of reflectance across the planet may be represented by a model in which the dominant scatterer is dust that absorbs in the ultraviolet and has an optical depth greater than 1. The atmosphere above the polar region is clearer than over the rest of the planet.*

Two major objectives of the ultraviolet spectrometer experiment are (i) measurement of the structure and composition of the upper atmosphere and (ii) photometric and spectral mapping of the lower atmosphere and surface of Mars (1). The upper atmosphere measurements are performed by observing the sunlit limb of the planet as the spacecraft motion causes the field of view of the instrument to pass through successively lower levels of the atmosphere. Measurements of the lower atmosphere are obtained by pointing the instrument directly at the area of the planetary disk that is being mapped. The Mariner 9 spectrometer is similar to those used on Mariners 6 and 7 and OGO-4 (2). During the first 30 days of the mission, the ultraviolet spectrometer measured the temperature and density of the upper atmosphere of Mars and discovered that this atmosphere, like the earth's, re-

sponds to changes in solar activity. The spectrometer also measured the spectral and photometric properties of the atmosphere during the protracted dust storm of 1971.

During the first 30 days, observations of the airglow above the bright limb of Mars made on 14 orbits were of sufficient quality to provide good altitude profiles. The principal spectral emissions observed during these limb crossings were those first measured in 1969 by the ultraviolet spectrometers on Mariners 6 and 7 (3): namely, the atomic hydrogen 1216-Å Lyman-alpha line; the atomic oxygen 1304-, 1356-, and 2972-Å lines; the atomic carbon 1561- and 1657-Å lines, the carbon monoxide A-X fourth positive and a-X Cameron bands, the ionized carbon monoxide B-X first negative bands, and the ionized carbon dioxide B-X and A-X bands. This Martian airglow is produced by the action of solar ultra-

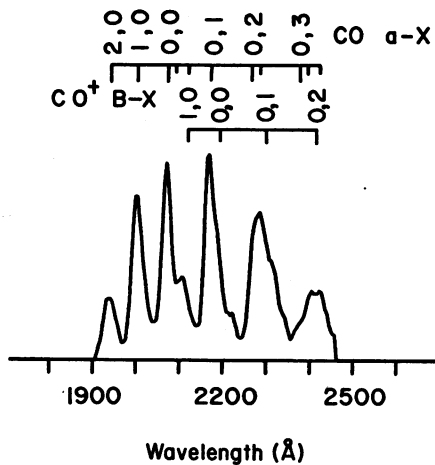


Fig. 1. Airglow spectrum of Mars between 1910 and 2460 Å. This wavelength interval, which contains the CO a-X Cameron bands and the CO⁺ B-X first negative bands, was used to obtain the emission rates shown in Fig. 3. This calibrated spectrum was obtained by summing 20 individual spectral observations, as was the spectrum in Fig. 2.

violet radiation on the atoms and molecules in the upper atmosphere of Mars.

The airglow spectrum of Mars in the 1910- to 2460-Å range contains the intense CO a-X bands and the weaker CO⁺ B-X bands as shown in Fig. 1. Figure 2 demonstrates that the CO A-X bands contribute most of the intensity in the 1420- to 1760-Å region, while the atomic carbon lines make a substantial contribution. Because the analysis of the Mariner 6 and 7 data showed that the most prob-

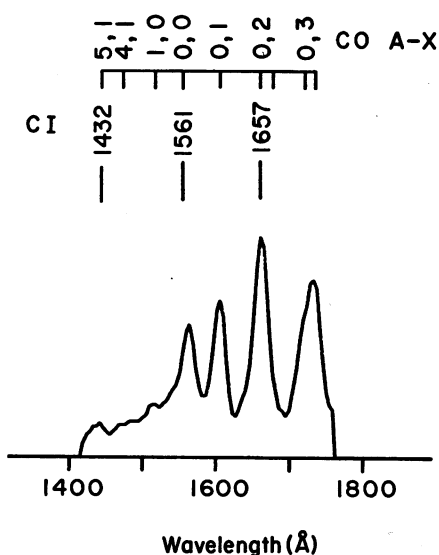


Fig. 2. Airglow spectrum of Mars between 1420 and 1760 Å. This wavelength interval, which contains the CO A-X fourth positive bands and the CI atomic carbon lines, was used to obtain the emission rates shown in Fig. 3.

able source of excitation of the carbon monoxide A-X and a-X bands is the electron and photon impact-induced dissociative excitation of carbon dioxide, the intensity of these bands as a function of altitude is used to determine the density distribution of carbon dioxide in the upper atmosphere of Mars (4). In turn, the scale height of these emissions is used to deduce the temperature of the upper atmosphere. The emission rate of these two band systems as a function of altitude is presented in Fig. 3 for a limb observation that was made on revolution (Rev) 34 on 1 December 1971, and is typical of the quality of the limb measurements made during the first 30 days.

An indicator of the amount of atomic oxygen in the atmosphere is the 1304-Å resonance line of atomic oxygen that appears in the airglow. The apparent emission rate of this line on pass 34 is plotted in Fig. 4. Because this emission line is optically thick in the Mars atmosphere, multiple scattering occurs and a radiative transfer analysis has to be performed to determine the atomic oxygen density (5).

The Lyman-alpha airglow line, which is a measure of the atomic hydrogen density in the Mars atmosphere, extends to great altitudes above the planet. The apparent emission rate of this line on Rev 34 was determined as a function of altitude and also is plotted in Fig. 4. Individual measurements were fitted with a straight line as shown. This emission line is also optically thick, although not as thick as the atomic oxygen line. To determine the exospheric temperature and density distribution of atomic hydrogen, it is necessary to analyze this emission along the entire orbit, which extends to an altitude of 17,000 km (6).

Parameters describing the limb crossings, relevant solar indices, and a summary of some preliminary results obtained from the limb data for the first 30 days are presented in Table 1. The solar indices are the Ottawa 10.7-cm flux index and the Zurich sunspot number; an approximate time adjustment has been made to allow for the nonzero angle between Mars, the sun, and the earth (7). The atmospheric quantities included in Table 1 are the scale height of the CO a-X bands and intensity of the Lyman-alpha line. The scale height is calculated in the 160- to 220-km region (4), and the 2 standard deviation error

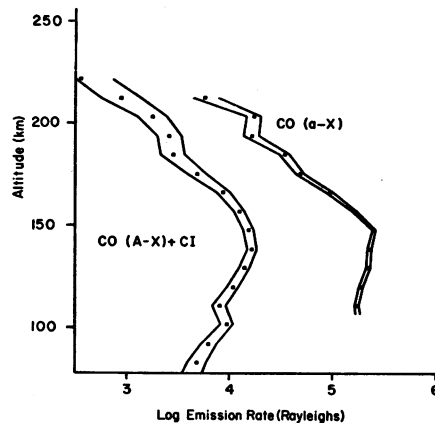


Fig. 3. Emission rates of the CO a-X Cameron bands and the sum of the CO A-X fourth positive bands and the atomic carbon lines as a function of altitude. The wavelength intervals used to obtain these two airglow profiles are shown in Figs. 1 and 2. Data points are dots; the envelopes represent ± 2 standard deviation error bars derived from counting statistics.

is on the order of ± 3 km.

Variations in the scale height are of particular importance because they are of sufficient magnitude to be statistically significant. They occur during a time of changes in the solar 10.7-cm flux, which is an indicator of the intensity of the solar radiations that ionize and heat the earth's upper atmosphere. It seems likely that the temperature of the upper atmosphere of

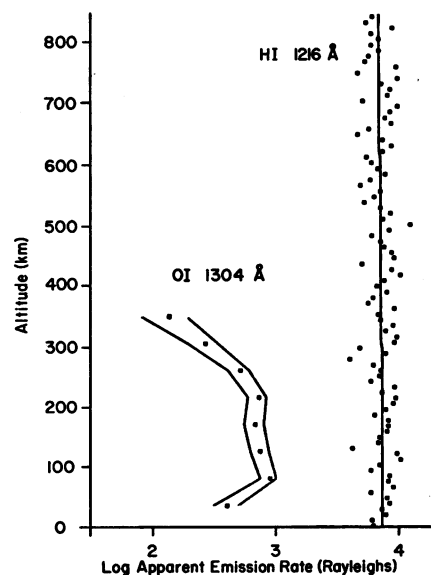


Fig. 4. Apparent emission rates of the atomic hydrogen 1216-Å line and the atomic oxygen 1304-Å line as a function of altitude. Data points are dots; the envelope around the 1304-Å data represents the ± 2 standard deviation error bars derived from counting statistics. The line through the 1216-Å data is a straight line fitted by a least-squares method.

Table 1. Airglow observations above the bright limb.

Rev	Limb crossing				$\cos \chi \dagger$	$\Delta Z \ddagger$ (km)	Scale height § (km)	10.7- cm flux	Lyman- alpha intensity ¶ (kR)	$R_z \#$
	Date	G.M.T.	Latitude* (°S)	Longitude* (°W)						
2	15 November	01:24	24	212	0.98	7.6	22	107	7.7	45
28	28 November	01:54	46	105	0.84	9.3	22	122	7.4	64
30	29 November	01:51	48	92	0.85	9.3	22	115	6.4	69
32	30 November	01:48	45	85	0.84	9.3	20	113	6.6	80
34	1 December	01:45	47	69	0.85	9.3	18	109	7.1	63
36	2 December	01:41	46	62	0.85	9.2	17	117	6.4	70
38	3 December	01:39	47	51	0.85	9.1	24	115	6.9	92
40	4 December	01:37	47	40	0.85	9.1	26	117	6.9	107
42	5 December	01:30	12	0	0.99	3.7	18	118	7.2	83
44	6 December	01:34	47	19	0.85	9.1	19	125	7.4	108
46	7 December	01:31	46	8	0.85	9.1	19	128	7.2	122
54	11 December	01:16	46	325	0.86	8.8	19	124	7.2	85
56	12 December	01:12	45	315	0.85	8.8	17	127	7.2	98
58	13 December	01:07	45	303	0.86	8.8	22	122	7.7	80

* Approximate. † Cosine of the solar zenith angle at the limb crossing. ‡ Altitude interval between successive spectra. § Determined from the CO a-X emissions. || Provisional Ottawa solar 10.7-cm flux index. ¶ At an altitude of 150 km. # Provisional Zurich sunspot number (7).

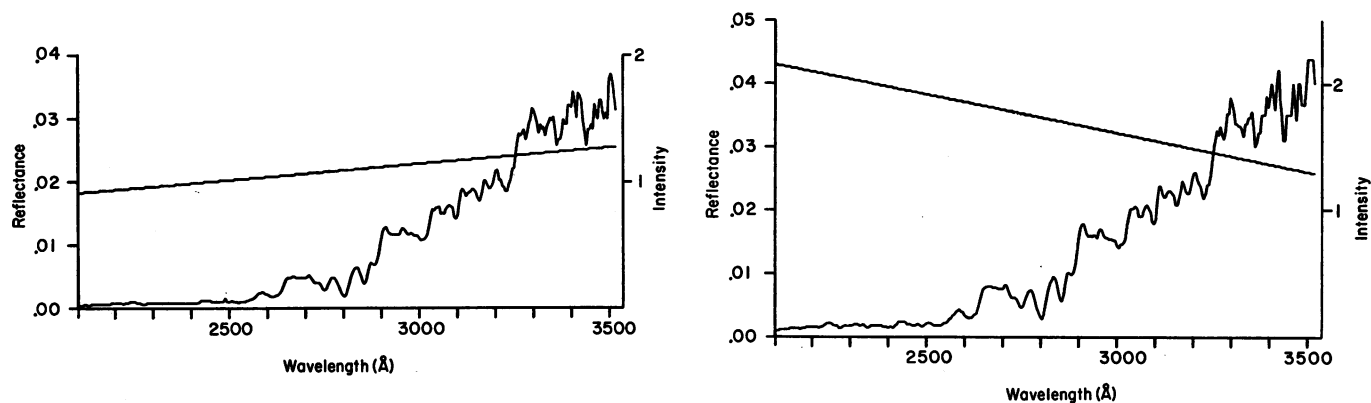


Fig. 5 (left). Ultraviolet reflectance in dusty region. The intensity of the ultraviolet spectrum observed on Mars near latitude 45°S in the orbital pass described in Fig. 7 when the illumination angle was 52°, the viewing angle 36°, and the phase angle 79° [units on the right-hand ordinate are 10^{13} photon $\text{cm}^{-2} \text{sec}^{-1}$ (15 \AA^{-1})]. Fig. 6 (right). Ultraviolet reflectance in polar region. The intensity and reflectance of Mars obtained near latitude 86°S on the revolution shown in Fig. 7 when the illumination angle was 65°, the viewing angle 59°, and the phase angle 38°.

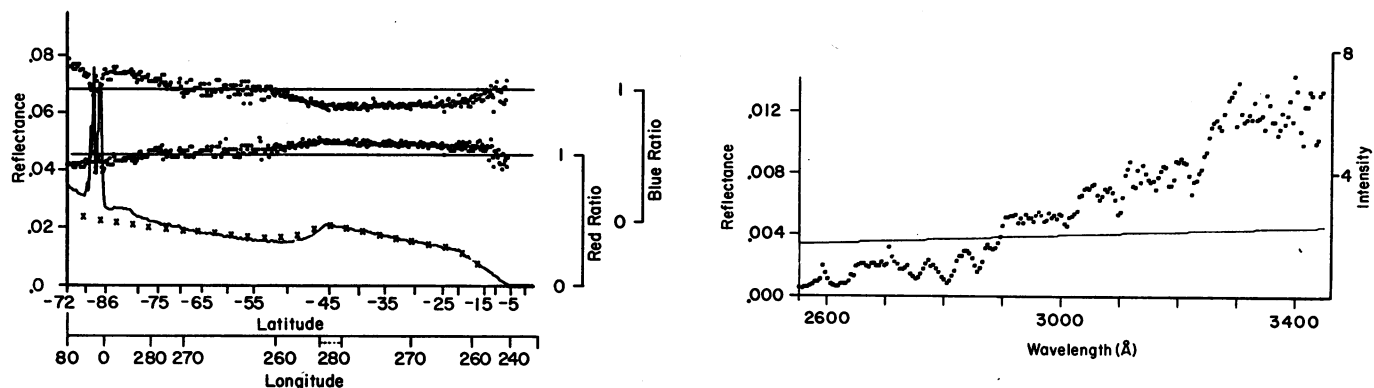


Fig. 7 (left). Reflectance at 3050 Å and blue and red color ratios for Rev 48 observations. The solid curve represents the reflectance measured in a 100-Å wide band centered at 3050 Å. Results of calculations with the model that has $\omega_0 \ll 1$ and $\tau \approx 1$ are indicated by the x symbols. The color ratios are plotted as dots for each spectral observation on the planet. The blue ratio is defined as the ratio of the reflectance measured at 2580 Å to that at 3050 Å, and the red ratio is the 3380-Å reflectance relative to the 3050-Å value. A value of 1 for the blue and red ratios is equivalent to the color of the sun. The blue ratio scale is displaced upward. Fig. 8 (right). Phobos ultraviolet reflectance. The relative spectral intensity and reflectance of Phobos obtained on Rev 48. Values of reflectance and intensity are lower limits [units on the right-hand ordinate are 10^{12} photon $\text{cm}^{-2} \text{sec}^{-1}$ (15 \AA^{-1})]. At the time of the observation, the sun-Phobos-instrument angle was 49°.

Mars is responding to changes in solar activity, but that it also is affected by atmospheric processes not necessarily connected with changes on the sun. The Lyman-alpha intensities seem to be correlated with the Zurich sunspot number, which has been shown to be an indicator of the intensity of the solar Lyman-alpha radiation (6). However, the variation in these intensities may reflect actual changes in atomic hydrogen densities in the Martian atmosphere.

These two observations demonstrate a curious result of space exploration. The Martian atmosphere is responding to changes in solar activity and the Mariner 9 ultraviolet spectrometer is detecting this response 3 days before the effects of the changes are felt in Earth's atmosphere.

Over the entire disk of Mars, except at the polar cap, the reflected spectrum is produced by the scattering of sunlight by molecules and particles in the atmosphere. In contrast to the spectra obtained by the Mariner 6 and 7 ultraviolet spectrometers in 1969, the spectral shape of the Mariner 9 reflectance depends on what particular location on the planet is being observed. While the details in the spectra of Mars originate in the solar spectrum, the overall spectral shape is determined by the relative amount of molecular or large particle scattering taking place. Two examples of Mars spectra are shown in Figs. 5 and 6 together with the reflectance as a function of wavelength. Reflectance as used in this report is defined as one-fourth the ratio of the intensity (photon $\text{cm}^{-2} \text{sec}^{-1} \text{\AA}^{-1}$) of the region of Mars being observed to the solar flux (photon $\text{cm}^{-2} \text{sec}^{-1} \text{\AA}^{-1}$).

The occurrence of the protracted dust storm on Mars has changed the characteristics of the ultraviolet reflectance from those observed by Mariners 6 and 7 in 1969 (8). The magnitudes of the reflectances are smaller than in 1969. When the measurements obtained by Mariners 6 and 7 and Mariner 9 at phase angles varying from 15° to 84° are extrapolated to 0° phase angle, the geometric albedo of Mars at 3050\AA in 1971 is 0.025 compared with 0.035 in 1969. This result indicates that the dust, which is dominating the ultraviolet light scattered from the disk of Mars, is a strong absorber in the ultraviolet.

A model to explain the observed variation of reflectance across the planet has been constructed with the use of the following information. The

low value of reflectance and lack of small-scale variations imply that the single scattering albedo of the dust particles, ω_0 , is small and that the optical depth, τ , is greater than 1. Marked deviations from this model for the reflectance and color ratios occur only near the south polar cap. Figure 7 demonstrates this result from data obtained on Rev 48. The increase in reflectance seen on the left side of Fig. 7 occurred when the spectrometer field of view crossed the south polar cap of Mars, indicating that the atmosphere is sufficiently clear for ultraviolet light to penetrate to the surface. During this orbit, a contiguous swath of reflectance data was obtained when the field of view crossed the polar cap and then moved northward. It may be seen in the figure that the model adequately explains the reflectance except in the south polar region where the reflected light intensity is larger than the model predicts. At this same location, the blue color ratio is high and the red color ratio low. These results indicate that there is an enhancement in the Rayleigh scattering contribution to the reflectance at this location and, hence, a decrease in the amount of dust in the atmosphere as compared to the rest of the planet. The increase in intensity in the south polar region is equivalent to a clear atmosphere of 1.4-mb pressure above the effective ultraviolet absorption level.

Several ultraviolet spectra of Phobos were obtained on Rev 48 during the spacecraft sequence that also produced two television pictures of Mars' inner satellite. One of these spectra in the wavelength region between 2550 and 3450 \AA is shown in Fig. 8. The absolute values of both the intensity and reflectance in the figure are lower limits set by assuming that Phobos was fully within the field of view of the spectrometer. Our current best estimate of the actual reflectance would double the scale given in Fig. 8. Its magnitude is still significantly less than that of Mars. The reflectance of Phobos decreases as the wavelength decreases from 3450 to 2550 \AA . The reflected light has essentially the same color as Martian dust (Fig. 5).

To summarize, in 30 days of orbital observations, the ultraviolet spectrometer measured the density distribution of the upper atmosphere of Mars and obtained the first observations of variations in this distribution as a function of solar activity. During this same period, the atomic hydrogen and

atomic oxygen airglows were present during each limb observation. Airglow intensities observed in this experiment are comparable to those observed in the Mariner 6 and 7 experiment in 1969.

In sharp contrast to the upper atmosphere observations, the lower atmosphere of Mars is different in 1971 from what it was in 1969. Mariner 6 and 7 found a clear atmosphere in which molecular scattering determined the ultraviolet reflectance. The ultraviolet reflectance measured by Mariner 9 is dominated by particle scattering. The atmosphere above the polar region is clearer than that over the rest of the planet.

CHARLES A. BARTH

CHARLES W. HORD, A. IAN STEWART
*Department of Astro-Geophysics and
Laboratory for Atmospheric and Space
Physics, University of Colorado,
Boulder 80302*

ARTHUR L. LANE

*Space Science Division, Jet Propulsion
Laboratory, California Institute of
Technology, Pasadena 91103*

References and Notes

1. C. W. Hord, C. A. Barth, J. B. Pearce, *Icarus* 12, 63 (1970).
2. C. A. Barth and E. F. Mackey, *IEEE Trans. Geosci. Electron.* GE-7, 114 (1969); J. B. Pearce, K. A. Gause, E. F. Mackey, K. K. Kelly, W. G. Fastie, C. A. Barth, *Appl. Opt.* 10, 805 (1971).
3. C. A. Barth, W. G. Fastie, C. W. Hord, J. B. Pearce, K. K. Kelly, A. I. Stewart, G. E. Thomas, G. P. Anderson, O. F. Raper, *Science* 165, 1004 (1969); C. A. Barth, C. W. Hord, J. B. Pearce, K. K. Kelly, G. P. Anderson, A. I. Stewart, *J. Geophys. Res.* 76, 2213 (1971).
4. A. I. Stewart, *J. Geophys. Res.* 77, 54 (1972).
5. G. E. Thomas, *J. Atmos. Sci.* 28, 859 (1971); D. J. Strickland, G. E. Thomas, P. R. Sparks, in preparation.
6. D. E. Anderson, Jr., and C. W. Hord, *J. Geophys. Res.* 76, 6666 (1971).
7. We thank Professor M. Waldmeier of the Swiss Federal Observatory, Zurich, for providing provisional sunspot numbers in advance of publication of his data. On 30 November, because of the relative positions of Mars, the earth, and the sun, solar features lying on the sub-Earth meridian had lain on the sub-Mars meridian 3.0 days earlier. The position of the solar indices in Table 1 takes account of this 3-day correction. More precise corrections, 2.4 days for the Ottawa 10.7-cm flux index and 2.8 days for the Zurich sunspot number, would take account also of the different G.M.T. appropriate to the limb crossing (0200), the Ottawa index (1700), and the Zurich number (0600 to 0900). The corrections increase by about 1 day per month.
8. C. A. Barth and C. W. Hord, *Science* 173, 197 (1971); C. W. Hord, *Icarus*, in press.
9. In addition to ourselves, the ultraviolet spectrometer team consists of R. C. Bohlin, R. L. Davis, M. L. Dick, L. R. Dorman, P. E. Evans, R. A. Goette, K. K. Kelly, A. H. Lineberger, G. G. McNutt, K. D. Pang, J. B. Pranke, L. H. Parmelee, S. Schaffner, K. E. Simmons, D. M. Stern, and D. J. Strickland at the University of Colorado; and J. M. Ajello, J. W. Farrar, and R. F. Ebbett at the Jet Propulsion Laboratory. This research was sponsored by the National Aeronautics and Space Administration.

27 December 1971